EUROPEAN ORGANIZATION FOR NUCLEAR RESEARCH

CERN-ACC-NOTE-2022-0016
NIMMS – Note – 009

Mariusz.Sapinski@cern.ch

PRELIMINARY DESIGN OF SEEIIST HIGH ENERGY BEAM TRANSFER LINES

*M. Sapinski**

*SEEIIST Association, Geneva, Switzerland and CERN, Geneva, Switzerland
Currently at Paul Scherrer Institute, Villingen, Switzerland

Abstract

The South East Europe International Institute for Sustainable Technologies (SEEIIST) is planning to construct a new Carbon Ion Radiation Center in South East Europe. This new facility will have an experimental program much more developed than the existing European carbon therapy centers. Therefore its High Energy Beam Transfer lines, which transport the beam from the extraction of the synchrotron to the patients or experiments, feature a larger experimental area which is well separated from the treatment area. Treatment rooms will need to be large to host additional medical equipment. The proposed beamline configuration foresees three treatment rooms: one with a horizontal beamline, one with horizontal and vertical beamlines, and one with a gantry. Additional rooms may be added in the future. The new facility will not be constrained by space, however, it is important to keep its complexity and overall cost limited. With a total length of around 200 meters, the beamlines will transport the beam using a relatively small number of magnets, nevertheless keeping the beam envelope narrow and with minimal losses and allowing for various extraction configurations. The final segments of each beamline will minimize the beam divergence and regulate the beam spot size on the patients or the experiments.

CERN-ACC-Note-2022-0016, NIMMS-Note-009

28 June 2022
mariusz.sapinski@cern.ch

Preliminary design of SEEIIST High Energy Beam Transfer lines

Mariusz Sapinski *
SEEIIST and CERN, CH-1211 Geneva, Switzerland

Keywords: beam transfer lines, ion therapy, CIRT

Summary

The South East Europe International Institute for Sustainable Technologies (SEEIIST) is planning to construct a new Carbon Ion Radiation Center in South East Europe. This new facility will have an experimental program much more developed than the existing European carbon therapy centers. Therefore its High Energy Beam Transfer lines, which transport the beam from the extraction of the synchrotron to the patients or experiments, feature a larger experimental area which is well separated from the treatment area. Treatment rooms will need to be large to host additional medical equipment. The proposed beamline configuration foresees three treatment rooms: one with a horizontal beamline, one with horizontal and vertical beamlines, and one with a gantry. Additional rooms may be added in the future. The new facility will not be constrained by space, however, it is important to keep its complexity and overall cost limited. With a total length of around 200 meters, the beamlines will transport the beam using a relatively small number of magnets, nevertheless keeping the beam envelope narrow and with minimal losses and allowing for various extraction configurations. The final segments of each beamline will minimize the beam divergence and regulate the beam spot size on the patients or the experiments.

*currently at Paul Scherrer Institut, Villigen, Switzerland

Contents

1 Introduction

The beam extraction from a synchrotron [1] is done by deviating the beam particles using a thin electrostatic septum magnet (ES). After receiving the transverse kick, the beam particles are still traveling in the same vacuum chamber as the circulating beam. The rotation of the beam ellipse in the phase space by $\pi/2 + n\pi$ maximizes the separation of the extracted particles from the circulating orbit, therefore the magnetic septum magnet (MS), with a blade thickness of the order of 10 mm, is located at this phase advance with respect to ES. After magnetic septum the extracted beam travels in a separate vacuum chamber and through different magnets, belonging to High Energy Beam transfer lines (HEBT).

Defining where exactly the HEBT starts is a matter of convention. Here, the optics calculations are performed starting at the face of the ES, as this is usually where the slow extraction simulations in the synchrotron ends. The disadvantage of this approach is that it is sensitive to potential modifications of synchrotron optics and resonant conditions, e.g. sextupole settings. However, this disadvantage is not critical, because the proposed beam-lines contain more degrees of freedom than constraints and can be adapted to different synchrotron optics.

The role of HEBT is to transport the beam and to form it according to experimental or medical requirements. The beam at the patient, or experimental target, should have required spot size and divergence. This translates to four Twiss parameters, two dispersion values and two dispersion derivatives: $\beta_{\mathrm{H}}, \alpha_{\mathrm{H}}, \beta_{\mathrm{V}}, \alpha_{\mathrm{V}}, \mathrm{D}_{\mathrm{H}}, \mathrm{D}'_{\mathrm{H}}, \mathrm{D}_{\mathrm{V}}, \mathrm{D}'_{\mathrm{V}}$. For optimal therapeutic beam all the above parameters, except β_{H} and β_{V}, should be zero. However, as described later, the

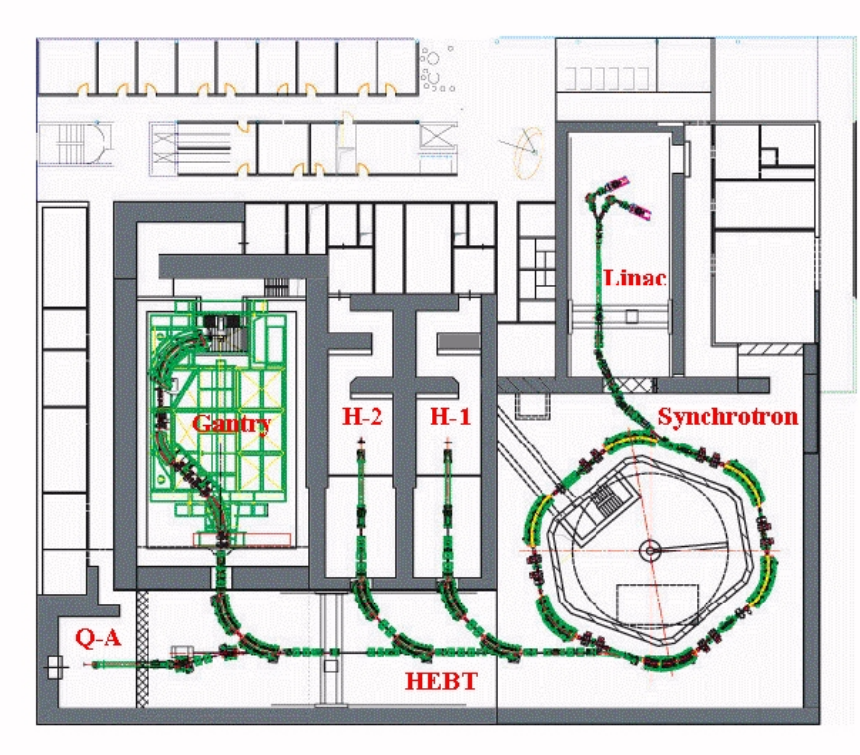

Figure 1: Layout of Heidelberg Ion Therapy Center (HIT). Figure from [2].

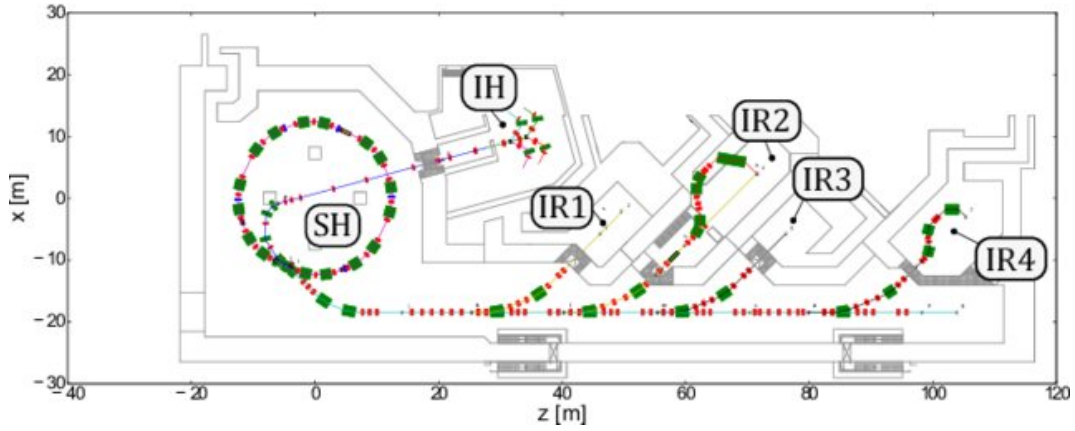

Figure 2: Layout of MedAustron facility. Figure from [3].

slow extraction process generates a beam with a specific shape of ,,bar of charge" and this leads to additional constraints on the horizontal phase advance between the ES and the patient or experiment.

The two main approaches to HEBT design are represented by the Heidelberg Ion Therapy Center (HIT) and MedAustron (Wiener Neustadt, Austria). The layout of HIT is shown in Figure 1. The design follows a strong space constraint (a footprint of about 80×60 meters) since the facility has been built inside the existing clinic campus. The bending angle of the HEBT dipoles is 45° and the number of quadrupoles of the shortest beam line is equal to the number of parameters that must be constrained (in this case 6; in the horizontal beam line the vertical dispersion and dispersion derivative are zero).

The considerations present in MedAustron HEBT design, which is shown in Figure 2, are quite different. First of all the were no strong space restrictions, so the overall footprint is more than 30% larger (about 140×45 meters) than HIT. The bending angle of the HEBT dipoles is half that of HIT (22.5°) and the design follows what has been proposed in the CERN Proton Ion Medical Machine Study (PIMMS) [4]. For instance, a single module, called phase-shifter-stepper, made of 6 quadrupoles, defines the beam size for all beamlines. There is also a rotator module that facilitates gantry installation and operation. The original concept of PIMMS is shown in Figure 3.

The HEBT of Centro Nazionale di Adroterapia Oncologica (CNAO, Pavia, Italy), due to specific space constraints, follows a different design. After extraction, the beam can be directed to a single vertical beamline. If the beam stays horizontal, it is directed to one of the three therapy rooms using a three-way switching dipole. Thanks to this solution the HEBT, shown in Figure 4, is short. However, the three-way switching dipole is more cumbersome in operation than the two-way switching one. The vertical beamline is relatively long, as it must stretch above a long horizontal section with a three-way switching dipole. The vertical beamline in MedAustron does not extend over a large segment of horizontal beamlines; therefore, this design is more adapted to the SEEIIST layout.

Finally, the Marburg Ion Therapy Center (MIT), employs familiar two-way switching 22.5° dipoles. It features a semi-vertical, 45° beamline instead of 90°one. The other centers, especially in Japan, use typically two-way switching dipoles and often feature multiple vertical beamlines: for example, Gunma University Heavy Ion Medical Center [6] has three

vertical beamlines (two for treatment and one for experiments), Kanagawa (i-Rock) has two [7], and Osaka facilities have two vertical beamlines and one 45° beamline [8].

2 Design concepts

The preliminary layout of the SEEIIST HEBT is presented in Figure 5 of [10]. Here, this initial design is upgraded, refined and described in detail. The main tool used to calculate optics solutions and generate survey files is MAD-X [11]. The plots were generated using python pyplot module.

The general concept is shown in Figure 6. Its main feature is a clear separation of treatment and experimental areas. Many radiobiological experiments are performed on large animals and should be invisible to patients. The separation is done along the principal beamline. The consequence is having left and right bending dipoles. This and the other aspects are discussed in the following subsections.

2.1 Bending and switching dipoles

The maximum energy of the PIMMS design is 400 MeV/u, which corresponds to a rigidity of 6.35 Tm. In the maximum field 1.5 T the bending radius is 4.23 m and the minimum length of the dipole is 1.661 m. Indeed the length of the PIMMS synchrotron dipole [4, 12]

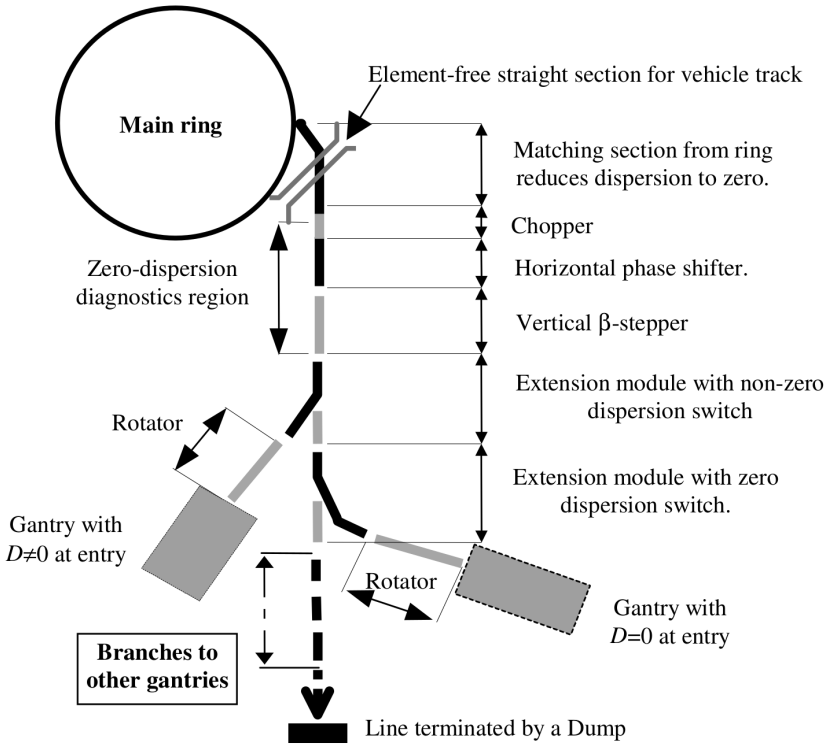

Figure 3: Layout of HEBT as originally proposed by PIMMS [4] (Fig. 9.1)

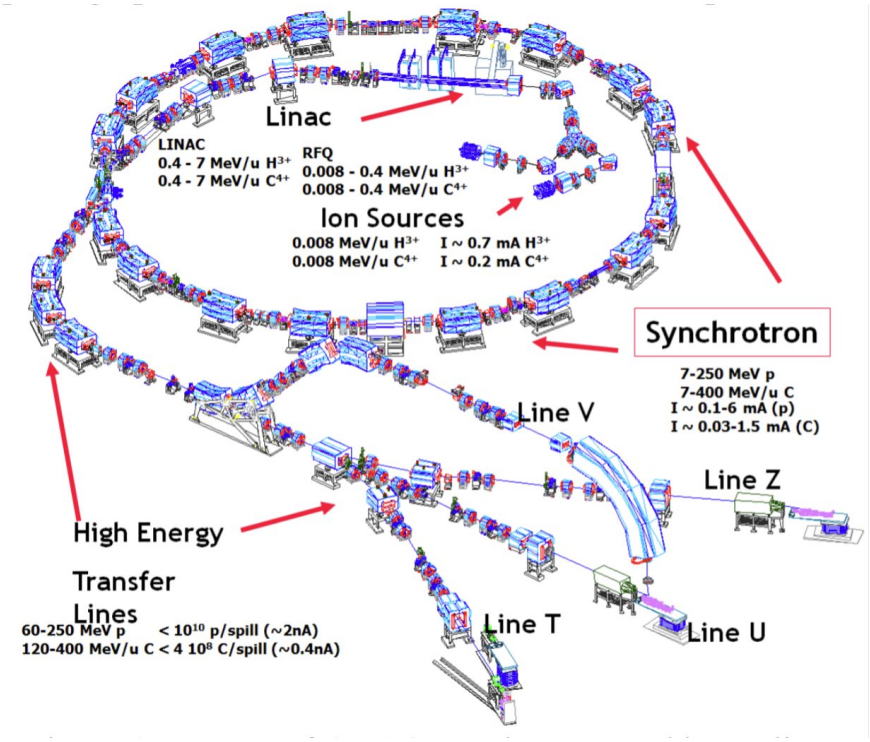

Figure 4: The CNAO layout with 3-way switching magnet, vertical beam line and three treatment rooms. Figure from [5].

is 1.662 m and for higher energies, the field is increased above 1.5 T, where the magnetic saturation leads to a nonlinear hysteresis curve.

In this study, the HEBT dipoles (both bending and switching) have the same length as PIMMS synchrotron ones, what allows to reduce the cost and complexity of the facility. However, there is enough space to make the SEEIIST HEBT dipoles longer. The following arguments support different designs of HEBT dipoles:

- HEBT work in quasi-DC mode, therefore the power consumption follows different

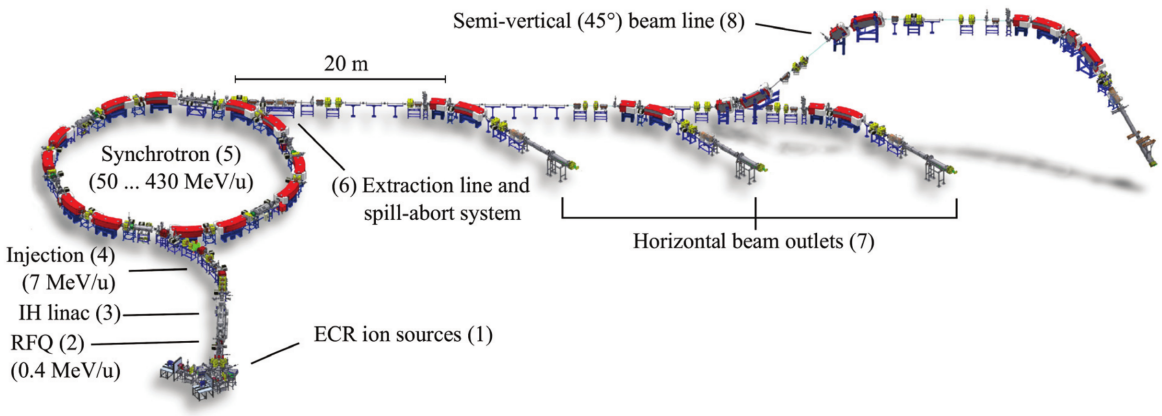

Figure 5: The MIT layout with one semi-vertical beam line. Figure from [9].

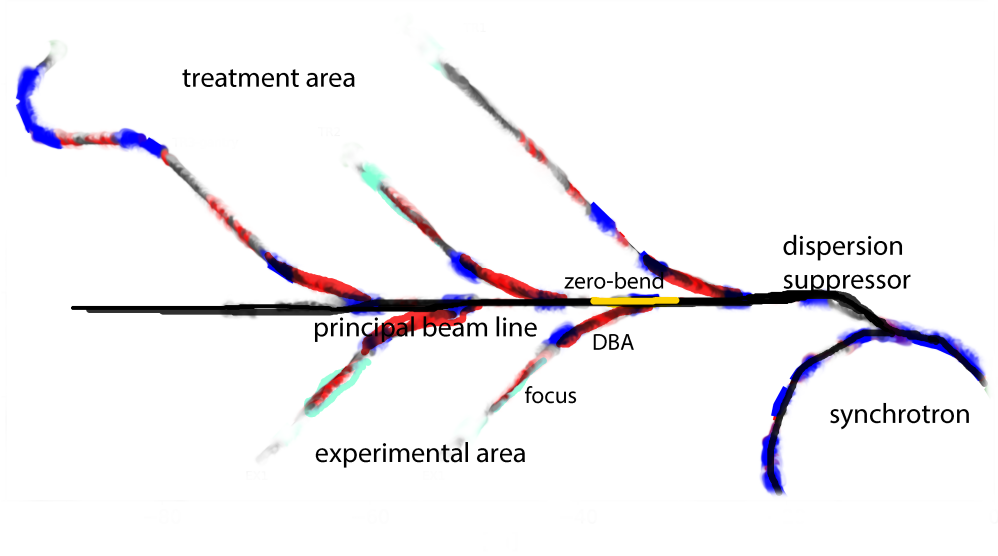

Figure 6: The general concept of SEEIIST HEBT.

pattern than in pulsed synchrotron; the magnets' coils could be designed with smaller electrical resistance;

- Because of relaxed space constraints the magnets could be longer and feature smaller maximum field, leading to smaller power consumption;
- HEBT is a single pass structure, therefore the quality of the magnetic field, in particular higher-order field components, can be relaxed.

This kind of considerations led MedAustron to design HEBT dipoles with length of 1.994 m and maximum field of 1.29 T [13].

A choice of two-way switching dipoles has been made in order to keep similarity to synchrotron dipoles and to use only unipolar power converters (in case of 3-way switching magnet the power converter must be bipolar), what decreases complexity and increases safety of the system (wrong polarity will not lead to sending the beam to a different treatment room). However it shall be noted that 3-way switching dipoles would allow to make HEBT more compact.

The SEEIIST dipoles in MAD-X are modeled as follows:

```
SBEND, ANGLE = -22.5*pi/180, L=1.664, E1 = -22.5*pi/180/2.0,
E2 = -22.5*pi/180/2.0, APERTYPE=rectangle, APERTURE={0.06, 0.03};
```

2.2 Quadrupole magnets

The HEBT quadrupoles must be stronger than synchrotron quadrupoles. The approach to the design of those magnets is similar for PIMMS, HIT and MedAustron. The maximum gradient in the PIMMS design is 19.67 T/m [12], HIT quadrupoles are slightly weaker:

19.3 T/m [14] and MedAustron uses quads with 18.9 T/m gradient. The length of the PIMMS quadrupole is 0.538 m, while HIT has quadrupoles of 0.519 m.

Here, we assume a quadrupole with length of 0.53 m and maximum normalized strength of $k_{1,max} = 3.0\ m^{-2}$ that corresponds to a gradient of 19.6 T/m. These magnets are defined in MADX as:

```
quadrupole, l = 0.53, apertype=circle, aperture={0.035};
```

The beam size reaches its maximum in the quadrupoles, therefore the aperture is critical in these magnets. In some cases the Twiss β functions can reach high values (more than 100 meters) especially in the last part of the beamline, where the beam is focused. In these areas, a star-shaped vacuum chamber, as described in [15], could be installed, leading to a significant increase in the available aperture.

In the further studies some of the quadrupoles could be identified as not requiring high gradients and could be replaced by smaller and cheaper MEBT quadrupoles. This approach, mentioned already for PIMMS, could reduce the overall cost of the facility without increasing the complexity.

2.3 Size of treatment rooms

The treatment rooms contain the beam line nozzle with the detectors of the dose delivery system which measure beam position and intensity, the robotic couch and the patient positioning system. It also usually contains a computer tomography scanner, which registers 3D images of the tumor in the position where the patient is irradiated. With the progress of medical diagnostic technology, additional devices such as Positron Emission Tomography (PET) scanners or Magnetic Resonance Imaging (MRI) scanners are installed in the treatment rooms. Therefore, the rooms of the future facility should be designed with a generous surface.

In current facilities, the widths of the rooms vary from 5.5 m (HIT) to about 8 m (MIT). HIT reported that their rooms are too narrow to fit modern medical diagnostic equipment [16]. For this reason, SEEIIST treatment rooms are specified with an ample width of 9.5 m.

The rooms are shielded from the accelerator by a 3-meter concrete wall, and usually all the magnets (except fast scanning magnets) are installed behind it. The 3-meter shielding wall separates also the rooms one from another *. Therefore, the distance between the following beam splitting points (splitting in the same direction) is:

$$L_{split} = (9.5 + 3.0)[m]/cos(45^\circ) = 17.68[m] \quad (1)$$

Although this is a large distance, keeping it will allow future reconfiguration of the treatment area and, for instance, a conversion of the fixed beam lines into additional gantries.

*The 3-meter side-shielding requirement can be relaxed for the wall between TR1 and TR2 because the beam never goes in the direction of the separating walls.

2.4 Order of beam lines

The beam lines to the irradiation rooms can be divided into horizontal, vertical and the one with gantry. In many facilities the vertical line is replaced or complemented by 45° line. Examples of such facilities are MIT and it's sister facility Shanghai Proton and Heavy Ion Center (SPHIC) which do not have any vertical beam line. The 45°beamline should be considered for the final design of the SEEIIST HEBT, because it is more compact and easier to build using standard dipoles. However, the therapeutic advantages and disadvantages are not discussed here and for now the vertical beamline from MedAustron is assumed.

In most facilities the first treatment room contains only the horizontal beam line. This beam line is the shortest in the facility therefore, it contains the smallest number of quadrupole magnets (for instance, in HIT the first beam line contains only 6 quadrupoles) what limits its configuration capability. Therefore, for SEEIIST we propose that the first treatment room be served by both horizontal and vertical beam lines. The vertical beamline contain vertical bends, therefore it is quite long allowing more space for the horizontal beamline.

2.5 Modularity

The HEBT lines are divided into modules (called here segments) with specific functions. For instance, the bending segment features a double bend achromat optics with a single quadrupole magnet in the center. It is the same for each of the beamlines, what greatly simplifies the facility operation and maintenance.

The concept layout of the facility's HEBT is shown in Figure 6. The segments are:

- dispersion suppressor,
- bending segment - double-bend achromat (DBA),
- zero-bend segment (which contains an inactive switching dipole),
- focusing segment.

The dispersion suppressor is the first HEBT segment and exists in only one instance. The DBA, zero-bend segment and focusing section are marked only once, but they are repeated as discussed in Section 4. The focusing module is designed to be the only module to be changed when the beam spot size on the patient has to be changed; however, more than one optics solution upstream of the focusing section is possible. This flexibility will allow to fine tune focusing if necessary.

2.6 Comparison to PIMMS

The proposed concept of SEEIIST HEBT is different from that of PIMMS. The main reasons for developing a new concept are:

- smaller footprint: PIMMS requires phase-shifter-stepper module which contains 6 quadrupoles to be installed after dispersion suppressor; in SEEIIST there is no such module, which allows to shorten the beam line before the first branching to TR1;

- similarly, in SEEIIST design, there is no rotator module, which helps to match the beam to the gantry;
- lack of these modules reduces the number of quadrupoles and leads to a less expensive facility;
- the focusing is done in focusing section, in principle the switching to different beam line can be faster and less complex, because it only requires switching the state of a single dipole;
- PIMMS concept is optimized for slowly extracted beams featuring bar of charge (hence phase-shifter-stepper module), SEEIIST concept can easily accommodate fast extracted beams and even smoothly switch between various extraction modes.

The PIMMS HEBT concept is genuine; however, currently only one facility, MedAustron, implements. All other facilities use more economical approaches, which require shorter beamlines and fewer magnets.

3 Beam parameters at extraction

The beam extraction is performed using resonant slow extraction process, however in the SEEIIST facility, a fast extraction scheme will be also implemented. In this study, the extraction conditions have been adapted from the design of the PIMMS synchrotron. The beamlines are flexible and can be adapted to different parameters of the extracted beam.

Table 1: Beam specifications at the entrance to electrostatic extraction septum. For horizontal emittance of the extracted beam see text.

parameter	**horizontal**	**vertical**
normalized emittance (Carbon, circulating beam)	$0.75\,\pi \cdot \mathrm{mm} \cdot \mathrm{mrad}$	$0.75\,\pi \cdot \mathrm{mm} \cdot \mathrm{mrad}$
normalized emittance (extracted beam)	$5\,\pi \cdot \mathrm{mm} \cdot \mathrm{mrad}$ (unfilled ellipse)	$0.75\,\pi \cdot \mathrm{mm} \cdot \mathrm{mrad}$
Twiss β	5.0 m/rad	6.523 m/rad
Twiss α	0	-0.17
dispersion D	1.942 m	0 m
dispersion derivative D'	-0.025	0.0

The beam parameters at the entrance to electrostatic septum are taken from page 165 of [4] † and are shown in Table 1. The beams in SEEIIST synchrotron, due to high intensities, are expected to have larger emittances than those reported in Table 1. However, because the multiturn injection takes place in horizontal plane, the increase of emittance is mainly expected in the same plane. This kind of asymmetric beams is present in the HIMAC

†Slightly different values are reported in Appendix 6 of [12], but the proposed beamlines are flexible and can be adapted.

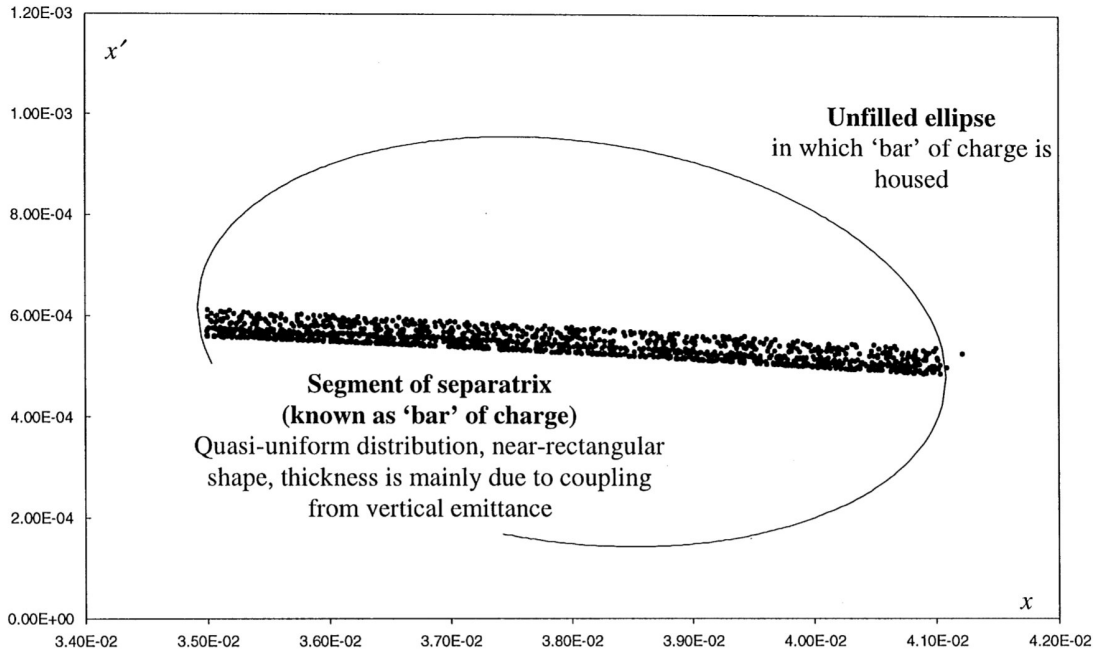

Figure 7: The ,,bar of charge". Figure from [17].

synchrotron, where the horizontal normalized emittance can be larger than $20\,\pi \cdot \text{mm} \cdot \text{mrad}$ while the vertical emittance remains about $1.1\,\pi \cdot \text{mm} \cdot \text{mrad}$. The emittance of the beam extracted in resonant slow extraction process does not depend on the emittance of the circulating beam. Therefore, assumption of the original PIMMS emittances (second row of Table 1) holds up.

In the horizontal plane the extracted beam phase space is not elliptical, it takes the form of a ,,bar of charge" (see [4], page 4 and Figure 7). The statistical emittance of such beam is very small (see, for instance, [18]). For such a beam shape in the phase space, the Twiss parameters are not well defined. To still use the linear optics code to design the beam lines, the same approach as in [4] is used. The ,,unfilled ellipse" is drawn around the ,,bar of charge" and the Twiss parameters are deduced from this ellipse. Because of this procedure the significance of horizontal Twiss parameters is different than in case of standard beams and one should remember that the way of calculation of the actual beam spot size is different. For example, using the Twiss parameterization of ,,unfilled ellipse", the beam spot size in the horizontal plane has an approximately rectangular distribution with a width of $2 \cdot \sqrt{\beta_H \epsilon_H}$ for the phase advance $n \cdot \pi$ with respect to the face of the electromagnetic septum (ES).

Until the entrance to the first magnetic septum, the beam parameters evolve following the ring optics. The Twiss parameters at the entrance to the Magnetic Septum (MS1) are shown in Table 2.

Table 2: Beam specifications at the entrance to the first magnetic extraction septum.

parameter	**horizontal**	**vertical**
Twiss β	20.1 m/rad	3.91 m/rad
Twiss α	-0.88	0.62
dispersion D	4.17 m	0 m
dispersion derivative D'	0.44	0.0

4 HEBT segments

The section of the synchrotron between the electrostatic (ES) and magnetic septa is where the extracted beam trajectory is still in the same vacuum chamber as the beam circulating in the sychrotron. The ES has a length of 0.8 meters and deflects the extracted beam by 2.5 mrad.

The center of the first magnetic septum (MS1) is 8.58 m downstream of the center of the electrostatic septum. The magnet has a length of 0.59 m and deflects the beam by 52 mrad. The second magnetic septum (MS2) has length of 0.84 meters and deflects the beam by 99.4 mrad. The distance from the center of the first magnetic septum to the second is 1.2 m. The first septum is ,,thin", i.e. the width of its blade is only 10 mm, while the MS2 is ,,thick" with blade width of 20 mm. Those magnets are described in [19].

The parameters and locations of the septa magnets have been proposed in PIMMS study and optimized in CNAO and MedAustron machines. The design of the HEBT after the MS2 is an original work done for SEEIIST project. In the following subsections, various segments of HEBT are discussed.

4.1 Dispersion suppressor segment

The dispersion suppressor is the first segment after extraction from the synchrotron. Its main function is to reduce to zero the values of the dispersion ($\mathrm{D_X}$) and dispersion derivative ($\mathrm{D_X^{'}}$). Suppressing the dispersion right after extraction is not strictly necessary, and, for instance, in HIT the dispersion is reduced to zero only at the patient's location. The advantages of suppressing the dispersion right after the extraction are:

- Minimization of horizontal beam size during further beam transport;
- Allowing for the beam emittance measurement, in the common part of HEBT beamlines, without uncertainties related to beam momentum spread;
- Simplification of HEBT lattice; in case when downstream beam lines branch into both, left and right sides, suppressing the dispersion after extraction reduces the number of quadrupoles needed downstream and allows the bending modules to have identical layout of quadrupoles independently on the bending direction.

The dispersion suppressor segment is also where a beam chopper is installed. This device is essential for patient safety [20] because it allows for a very fast beam abort. The chopper is made of four corrector magnets, which create a vertical or horizontal orbit bump around

an internal dump block. The beam size in the region of the dump should be small (i.e., small Twiss β and dispersion) to reach short beam abort times. Therefore, suppression of dispersion is important if the chopper bump is in the horizontal plane.

To suppress the dispersion, the segment must contain a dipole. The minimum number of quadrupoles is 2 because two parameters must be matched. The proposed layout of this segment is shown in Figure 8. The first two quadrupoles modify D_X and D'_X in such a way that they are suppressed in the downstream dipole. They also allow to keep the vertical Twiss beta function small (less than 10 m) and almost constant over 7 m distance, what is more than necessary to install a chopper[‡][20]. The last two quadrupoles prepare the beam for further transport, helping to avoid excessive Twiss β functions downstream. The total length of this segment, from the face of the first magnetic septum, is 14.2 m.

The Twiss β functions in the chopper location are minimized in both horizontal and vertical directions, minimizing the beam size in both planes (stigmatic focusing). However the dispersion is not yet zero there, leading to increase of horizontal beam size. The horizontal beam position is also affected by the setting of the extraction devices. For these reasons, it is suggested to have a vertical beam chopper.

Because of substantial space, larger than in PIMMS design, the chopper could be made of double chicane and double internal dumps. This solution, shown schematically in Figure 9, should significantly (up to a factor of 2) decrease the time required to abort the beam, which is currently about 200 μs. This limit is largely due to the time needed to change the field in the bumper magnets [21]. Double-chicane would allow to cut the beam tails on both sides simultaneously, leading to a shorter beam abort time, critical for FLASH therapy. Another idea worth investigating is the application of a RF-chopper, which becomes possible because

[‡]MedAustron chopper has length of about 5.2 m.

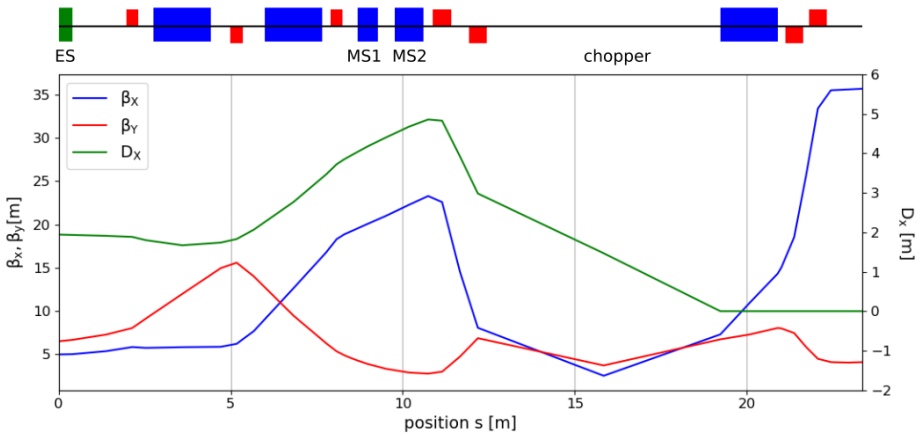

Figure 8: Proposed layout and optics of the dispersion suppressor segment. The green box at the beginning of the beam line is the electrostatic septum. The blue boxes are dipole magnets and the red ones are quadrupoles. The first two dipoles are still inside the synchrotron. The first magnetic septum is marked MS1 and the second one (MS2) follows it.

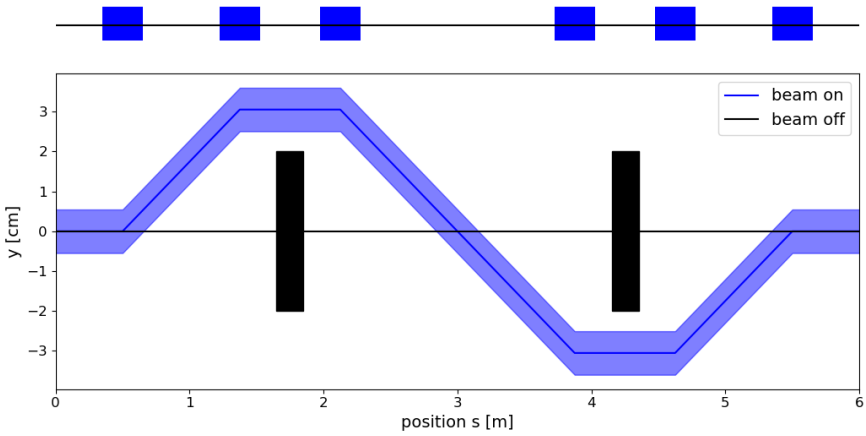

Figure 9: Chopper with double chicane and double dump. The kicker deflection angle is 2°. The beam envelope is calculated for carbon beam at 430 MeV/u.

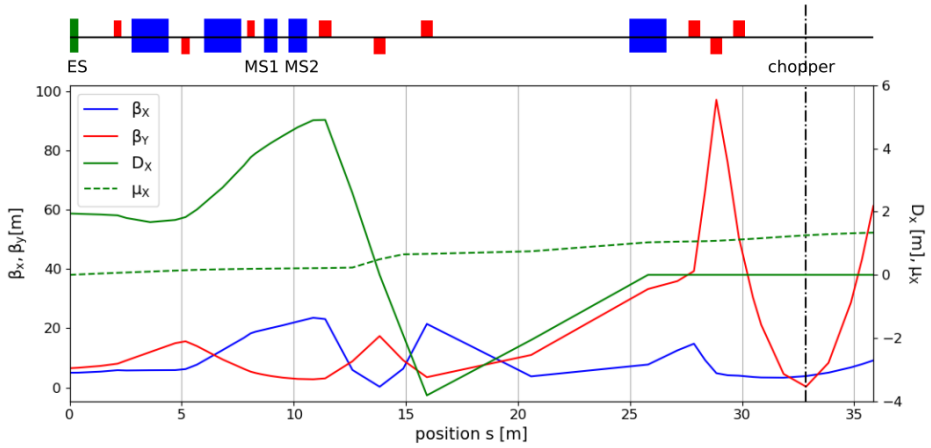

Figure 10: Dispersion suppressing section with bend in the right direction. The vertical dashed-dotted line is the center of chopper, where the phase advance is $5\pi/2$.

the RF-KO extraction works with a bunched beam.

The dispersion suppressor segment should be rich in beam instruments. In the chopper location at least two movable beam profile and position monitors should be installed to steer the beam through the chicane. Devices in this region should have proper radiation hardness due to beam losses generated on the dump blocks, but also radiation coming from the synchrotron extraction region. After the dipole additional instruments should be installed to measure beam size without contribution from dispersion.

The above layout of the dispersion suppressor bends the beam to the left, the same as the synchrotron magnets, as presented in Figure 11 (layout 1). The same bending direction was proposed in PIMMS and realised in MedAustron and CNAO. Bending in the opposite

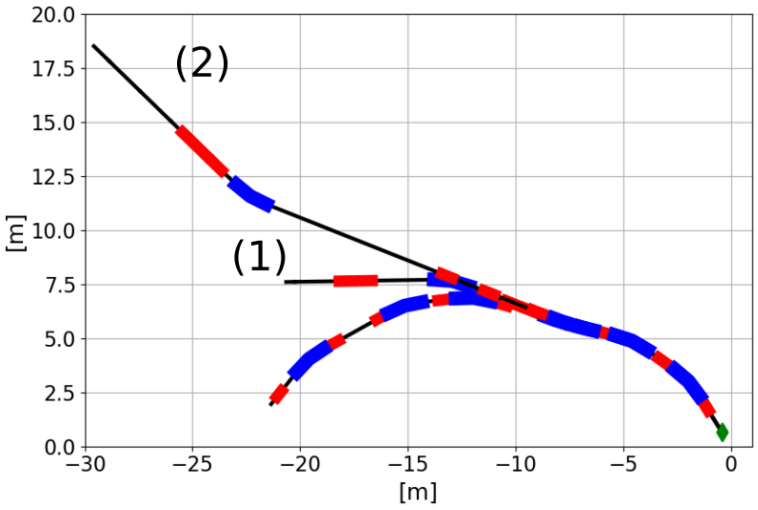

Figure 11: Proposed survey of dispersion suppressing segments. The beam, after extraction, is bend to the left (1) or to the right (2). In the second case, the length of the segment is much longer.

direction, as originally proposed for SEEIIST [22] (Figure 11 layout 2), means a necessity to change the dispersion polarity before the dipole. This requires more space and more quadrupole magnets than the left-bend solution. An example of a right-bend lattice is shown in Figure 10. The length of the segment is 27.5 m.

This particular solution features stigmatic focusing after the last triplet. The Twiss β in both directions have similar small values and the dispersion is 0. Due to the slow extraction process, as explained in Section 3, the horizontal beam emittance is much smaller than the vertical one and the beam phase space has the shape of ,,bar of charge". Furthermore, the horizontal phase advance with respect to ES can be tuned to exactly $5\pi/2$ with respect to the electrostatic septum, which, in theory, should allow exploration of the extremely small width of the ,,bar of charge". The resulting very small beam size in the location of the chopper could be used to further decrease the beam abort time. If this method of beam abort time reduction is used, the chopper bump must be horizontal.

The fine tuning of the phase space rotation to obtain a very small beam size may be difficult. In addition the slow extraction process may generate small horizontal movements of the beam which would be difficult to control and would outbalance the effect of small beam size on the speed of beam abort. These risks, together with the much longer length of the right-bending segment, lead to a choice of the left bending dispersion suppressor for further study.

4.2 Bending segment: double-bend achromat

After the dispersion suppressor sector the beam is transported in a common beam line to three treatment rooms, two experimental areas or straight to a beam dump. Five switching dipoles are installed in succession to direct the beam to a particular beam port. After each

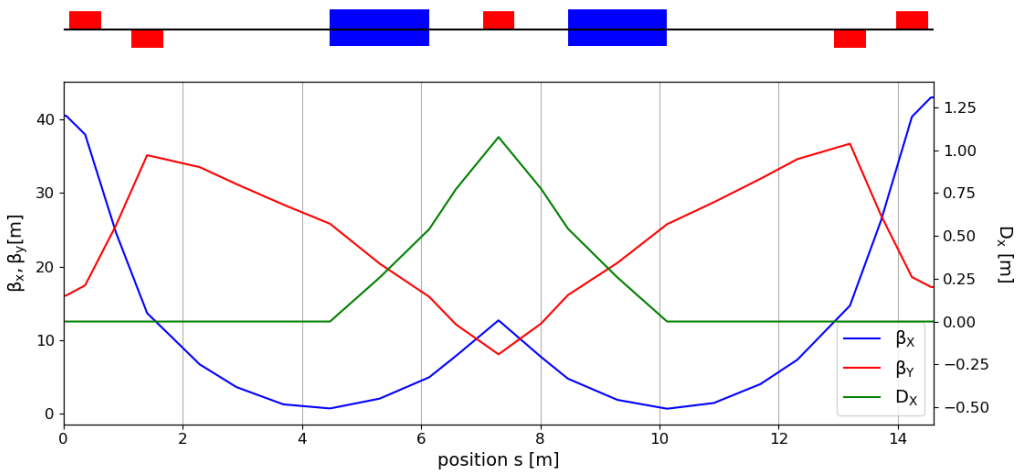

Figure 12: The Double-Bend Achromat segment with one central quadrupole, two side quadrupoles and left-bending dipoles.

switching dipole there is a second dipole magnet with identical bending angle in double-bend achromat (DBA) configuration. This allows us to close the dispersion generated by the switching dipole and arrive at the patient with $D_x = D'_x = 0$.

DBA segment is characterized by mirror symmetry, and the symmetry point is in the middle between the dipoles. The most common DBA variant has three quadrupoles between the dipoles, allowing for good control of vertical beam size. The solution proposed here, shown in Figure 12, is based on only one central quadrupole. This allows to shorten the DBA and limit the total number of quadrupoles needed in HEBT. And it still keeps the vertical Twiss β within reasonable limits.

The distance between the first two quadrupoles and the dipole is fixed by the requirement of the distance between the beam lines to the treatment rooms, as described in Section 2.3. The distance between the dipoles is minimized to decrease the overall length of the segment. The length of the DBA sector is 14.6 meters. Further shortening leads to difficulties in finding optics solution with reasonable beam sizes.

The layout foresees left and right bending sectors. Those sectors are identical; the only change is the sign of the bending angle and, consecutively, the sign of the dispersion produced.

4.3 Zero-bend transport

Zero-bend transport is a segment that contains two quadrupoles and an inactive switching dipole. Its function is to transport the beam on a straight path. When the dipole is active, the segment is a part of DBA and the two quadrupoles are used in matching DBA optics. In zero-bend configurations the role of the two quadrupoles is to keep beam envelope small during the transport along the principal beam line and prepare the Twiss parameters for the next DBA.

The length of the zero-bend (zbend) transport segment is 8.84 meters, and it is half of

L_{split} as defined by Equation 1 in Section 2.3. For each beam line, except TR1, one or more of the zero-bend transport segments allow to prolong the beam path until the DBA segment.

Each of zero-bend segments contain one vertical and one horizontal steerer magnet and a scintillating screen to measure beam position and size.

4.4 Beam focusing segment

The role of this segment is to prepare the beam for experiments or for patient treatment. Because the dispersion is suppressed in the upstream section (DBA), the medical requirements are simplified and a control of the following four Twiss parameters at the end of the beamline is required: $\beta_{\mathrm{x}}, \beta_{\mathrm{y}}, \alpha_{\mathrm{x}}$ and α_{y}. In addition, the solution should keep horizontal phase advance (μ_H) between ES μ_H far from $n\pi + \pi/2$, otherwise additional corrections to the beam size are needed. Therefore this section contains 4 quadrupoles.

The focusing segment contains two fast scanning magnets (horizontal and vertical) for pencil beam scanning delivery modality. The magnets, except for the scanning ones, are placed before a three-meter thick shielding wall. After the wall, the distance to the patient allows for installation of the nozzle with its monitors, and should be about 2 meters. It should also contain space to install a 3D-printed ridge filter, which will allow to deliver FLASH treatment [23].

The beam size on the patient is defined as Full Width at Half Maximum ($\mathrm{s_{FWHM}}$) should be regulated between 4 and 10 mm for energy range between 60 MeV (protons) and 430 MeV/u ($^{12}C^{6+}$). Smaller beam spots require overlapping of too many pristine Bragg peaks, leading to potential "hot spots". The Twiss α should be always close to zero to avoid position errors related to the estimate of the distance from the patient.

Because of resonant slow extraction mechanism and resulting differences in horizontal and vertical phase spaces, the regulation of the beam spot size on the patient is done differently in both planes. In vertical plane the Twiss β_{V} is defined as follows:

$$\beta_V = (s_{FWHM}/2.355)^2/\epsilon_{geom,V} = (s_{FWHM}/2.355)^2 \cdot \beta_r \cdot \gamma_r/\epsilon_{n,V} \tag{2}$$

The factor 2.355 is due to conversion between gaussian beam σ and the Full-Width-at-Half-Maximum ($\mathrm{s_{FWHM}}$). The normalized vertical emittance $\epsilon_{n,V}$ is given in Table 1, β_r is the speed expressed in units of light speed, and γ_r is the Lorentz factor.

In horizontal plane the particle distribution inside the ,,bar of charge" is approximately uniform, therefore there is not need for the conversion factor. The unfilled ellipse, which contains the ,,bar of charge", does not change with beam energy and corresponds to a fixed geometrical emittance $\epsilon_{\mathrm{geom,H}} = 5\pi$ mm mrad (see Table 1). Assuming infinitesimally narrow ,,bar of charge", the required Twiss β_{H} is described by an Equation 3, which is a result of a combination of ,,unfilled ellipse" equation and a straight line representing ,,bar of charge".

$$\beta_H^2 s_{FWHM}^2 tan^2 \mu_H - \beta_H \epsilon_{geom,H} + s_{FWHM}^2 = 0 \tag{3}$$

For phase advance μ_{H} close to $\mathrm{n} \cdot \pi$, where n = 1,2,3..., β_H varies between 3.2 m/rad for 4 mm beam spot and 20 m/rad for 10 mm spot. When μ_{H} is far from $\mathrm{n} \cdot \pi$, an additional matching of Twiss β is required to correct for the shape of the ,,bar of charge" projection is required. This correction is small for well-focused beams, but it can be quite large for 10 mm

Table 3: Vertical Twiss β functions on the patient for pencil beam scanning, for various beam conditions. The extreme values are in bold.

beam	$\beta_r\gamma_r$	$\epsilon_{geom,V}$	Twiss β_V for spot s_{FWHM}	
(particle, energy)	(relativistic)	$[\pi \cdot \text{mm} \cdot \text{mrad}]$	**4 mm**	**10 mm**
p, 60 MeV	0.362	2.05	**1.4 m/rad**	8.78 m/rad
p, 230 MeV	0.79	0.95	2.9 m/rad	17.9 m/rad
C, 100 MeV/u	0.476	1.57	1.8 m/rad	11.3 m/rad
C, 430 MeV/u	1.066	2.2	4.1 m/rad	**25.6 m/rad**

beam spot, where the unfilled ellipse is much larger in position than in angle. In general the phase advance of $\pi/2 + n\pi$ should be avoided, because a small variation of phase advance around these values leads to significant chance of the beam size.

Equation 3 is approximate because the real ,,bar of charge" has a complicated form, which cannot be well described by analytic formula. Detailed analysis and simulations of the slowly extracted beam with realistic phase space are needed to describe the horizontal beam shape on the patient. Those simulations should include the effect of beam scattering on the ridge filter, which is necessary for FLASH irradiation. The beam settings of each medically required beam must be commissioned before clinical use.

The extreme values of vertical Twiss β_V functions are calculated in Table 3, based on the normalized emittances of Table 1. In the following plots, the beam focusing optics is given for two extreme cases:

- $\beta_H = 3.2$ m/rad, $\beta_V = 1.4$ m/rad, for protons at 60 MeV and beam spot on patient of 4 mm,
- $\beta_H = 20$ m/rad, $\beta_V = 25.6$ m/rad, for $^{12}C^{6+}$ ions at 430 MeV/u and beam spot on patient of 10 mm.

The Figure 13 shows the example of the focusing segment. Length of the presented segment 10.6 m. The focusing segment of the beam line to TR1 must be longer, as explained in Section 5.1. Conversely, the beam line to the gantry could feature shorter focusing segment, as shown in Section 5.3.

This section transverses the shielding wall, i.e. the scanning magnets are already placed behind the shielding. Scanning magnets are more than 2 meters away from the isocenter (Source-to-Axis Distance, SAD $>$ 200 cm). Large SAD not only means comfortable patient clearance, but also improves the conformity of the delivered doses.

5 Beam lines

In this section the optics of the entire beam lines are discussed. Each beam line is composed of segments, which are explained in previous section.

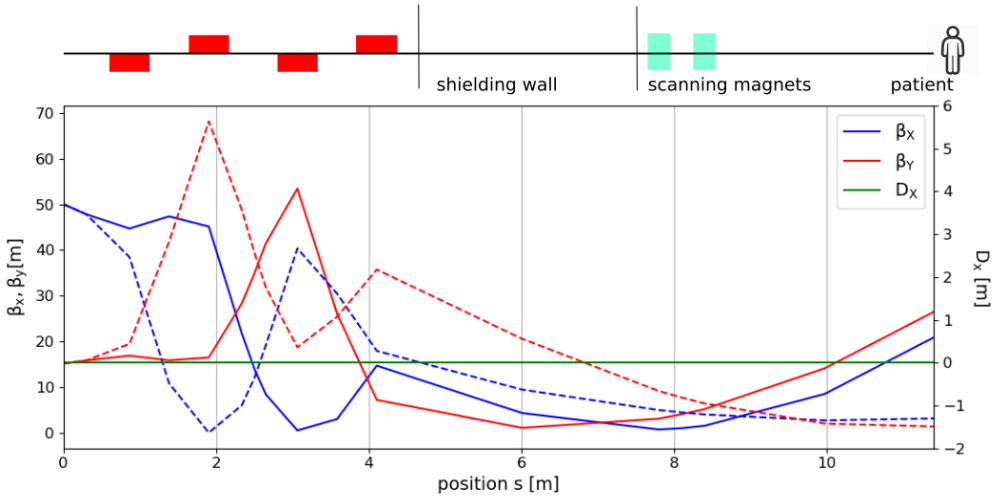

Figure 13: The focusing section with four quadrupoles, shielding wall and fast scanning magnets. Solid lines show Twiss β functions for 10 mm beam spot on patient for Carbon beam at 430 MeV/u. Dashed line show Twiss β functions for 4 mm beam spot on patient for proton beam at 60 MeV/u

5.1 Treatment Room 1 (TR1)

The first treatment room (TR1) is equipped with horizontal and vertical beamlines. Here, the vertical beamline design is borrowed from MedAustron. It has a length of 22.5 m from the start of the vertically switching magnet to the isocenter. The vertical beamline of the CNAO is much longer: 34 m, mainly because the three-way horizontal switching magnet must fit under it. The final bending dipole magnet in both facilities is 90°, which weighs approximately 70 tons.

A further study, done together with radiologists, will determine whether 90° beamline is necessary or if reaching the patient at 45° already fulfills medical requirements. The 45° beamlines are shorter and much cheaper to build and, as mentioned before, these kinds of beamlines are present in MIT and in several of the facilities in Asia.

The isocenters of both, the vertical and the horizontal beam lines, are in the same location. The beam focusing segment of the horizontal line is a longer than the focusing segment in other beamlines because the vertical line takes a lot of space. In this case the longer beamline makes the beam setup easier and requires less strength of the quadrupoles. The total length of this beamline, from ES to the isocenter, is 57.2 m. The length of the vertical beamline (not shown here) is 63.5 m.

The evolution of the Twiss β along the beam line is shown in Figure 14. Solid lines show Twiss β functions for beam spot size of 4 mm for 60 MeV protons, while dashed lines show the same for the 10 mm spot for C^{6+} beam at 430 MeV/u. The segments of the beam line are marked above. The first part, from ES to MS1, is where the extracted beam trajectory is still in synchrotron. DS is dispersion suppressor segment, DBA is the double-bend achromat and FOC is a long focusing section. The dark blue dipoles are active while the aquamarine

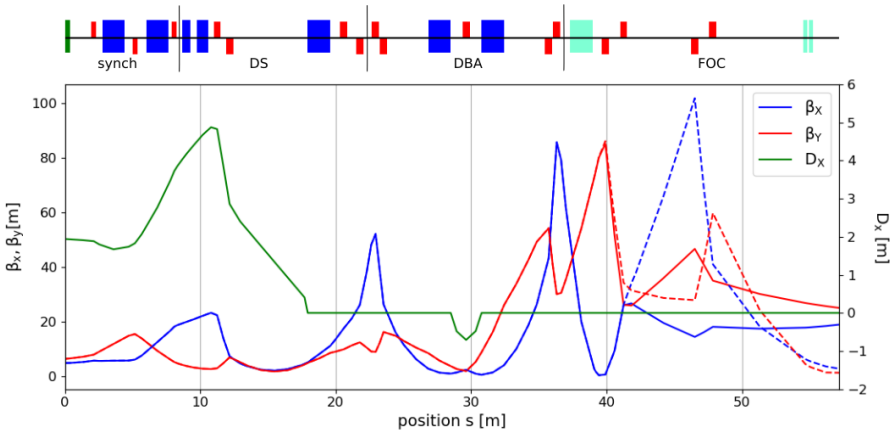

Figure 14: The optics solution for the horizontal beam line to TR1. The solid lines correspond to 430 MeV/u Carbon beam spot size on target of 10 mm, and the solid lines give the optics of a 60 MeV proton beam with beam spot of 4 mm.

ones are either non active for this beam path (as the first one in FOC section which is vertical switching dipole) or are scanning magnets.

5.2 Treatment Room 2

Treatment room 2 (TR2) features horizontal-only beamline which consists of dispersion suppressor, two zero-bend transport segments, DBA and focusing segment. The total length, from the ES to isocenter, is 65.8 m.

The Twiss β functions proposed for this beam line are shown in Figure 15. The solid line show focusing to get 10 mm beam spot on patient with 430 MeV/u carbon beam while dashed line show optics where the focusing section quadrupoles were set for 4 mm beam spot size with 60 MeV protons.

5.3 Treatment Room 3 (TR3) - gantry

The treatment room 3 (TR3) features a superconducting ion gantry, based on the proposal of TERA-CERN [24]. This gantry rotates by 200° and it is fixed to a thick wall. The gantry optics is design to reproduce on the patient the Twiss parameters at the handover point, which is located in front of the gantry. Therefore, the beam line optics must allow to control of Twiss parameters at this point.

The beam line to the gantry is the longest of the beam lines. It consists of dispersion suppressor segment, four zero-bend segments, double-bend achromat and a short focusing section with three quadrupoles (instead of normal four) and without scanning magnets, which are part of the gantry. The total length, from ES to the gantry handover point, is 80.9 m. Length of the gantry is about 25 m.

The Twiss functions of the proposed solution are shown in Figure 16. The plot shows the beta functions for extreme cases.

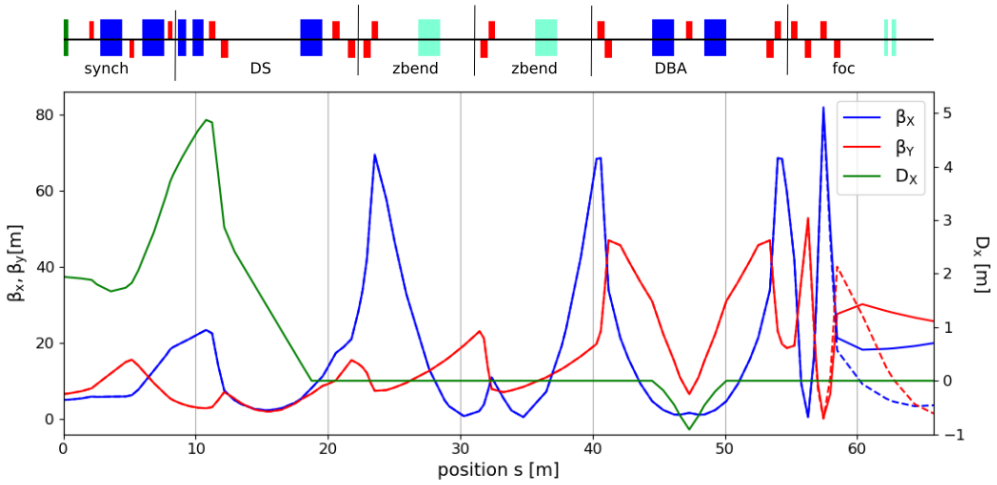

Figure 15: The possible optics solution for TR2. Solid lines correspond to the spot size of the 430 MeV/u carbon beam on a target of 10 mm. The dashed and dotted lines gives optics of 60 MeV proton beam with beam spot of 4 mm.

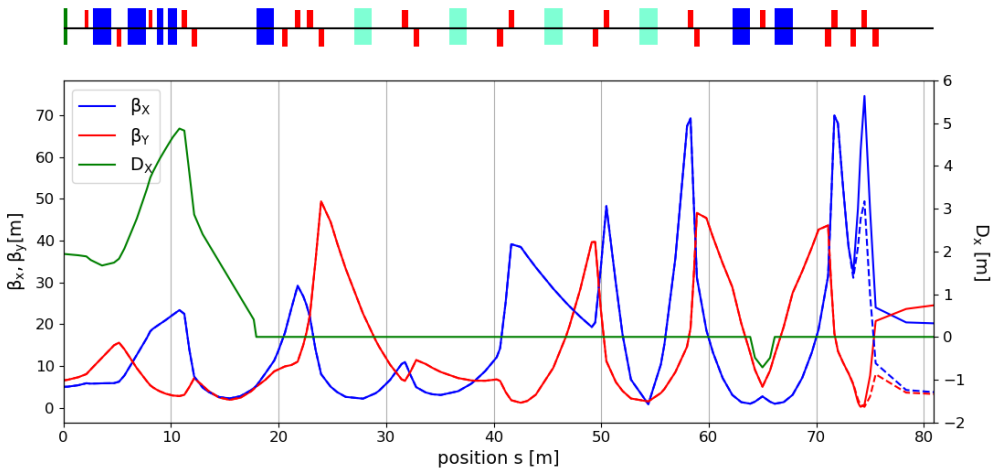

Figure 16: The complete optics solution for TR3 - up to the entrance to the gantry. Solid lines show Twiss β functions for the smallest required beam spot size (4 mm for the 60 MeV proton beam) and dashed lines for the largest (10 mm for the 430 MeV/u carbon beam).

5.4 Experimental beam lines

The two experimental beam lines (EX1 and EX2) direct the beam to a large and reconfigurable experimental area. Both beamlines are horizontal, however in the future a low-energy vertical beam line could be designed, as it is useful for certain types of experiments. Such a beamline has been suggested, for instance, for BioLEIR project [25]. Both beamlines feature

the same 4-quad beam focusing segment as the beam lines devoted to patient treatment. Therefore, they have the same capability to focus the beam as therapeutic beam lines.

The EX1 beam line is made of dispersion suppressor, one zero-bend segment, DBA, and a focusing segment. Its total length is 57 m. The optics functions for the two extreme focusing cases are shown in Figure 17.

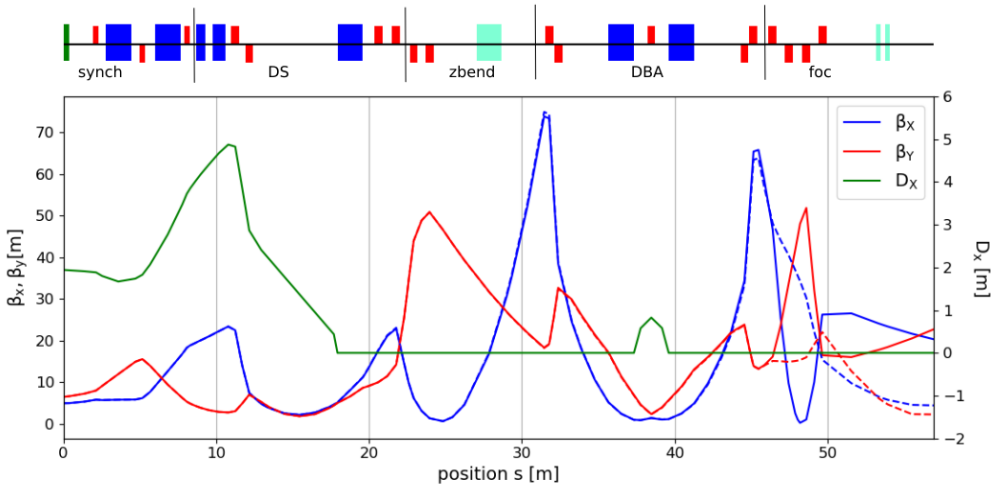

Figure 17: The beam optics solution for the first experimental beamline (EX1). The Twiss β functions are shown for a 4 mm beam spot with a 60 MeV proton beam (dashed lines) and for a 10 mm beam spot with a 430 MeV/u carbon beam (solid lines).

The optics settings of the second experimental beamline (EX2) are shown in Figure 18. This beamline had two additional zero-bend segments. Its total length is 74.6 m.

5.5 Beam dump

The beam which is not deviated to any of the treatment rooms or experimental ports can be dumped in the beam dump. Directing the beam to this beam dump is much slower than stopping it with the beam chopper, as the ramping down of the switching dipole takes hundreds of milliseconds. Therefore, this beam dump cannot be used as a patient safety device. Instead, it could be also used as an additional experimental area; however, in the current lattice configuration, the possibilities to freely focus the beam are limited.

6 Vacuum system

To avoid beam losses and scattering with the rest gas, the vacuum level in the HEBT must be better than 10^{-7} mbar. In case of vacuum leak, the segmentation of the vacuum system should allow operation of the largest possible part of the facility. To achieve this, the sector valves should be installed after each switching dipole, on both exiting beam lines. The exception is the last switching dipole, where a single vacuum valve can be installed on the

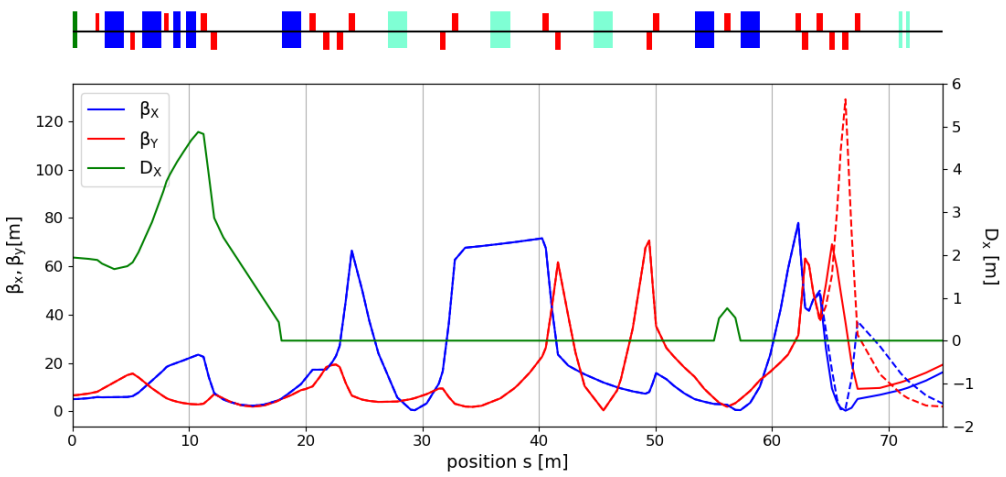

Figure 18: The beam optics solution for the second experimental beamline (EX2). The Twiss β functions are shown for a 4 mm beam spot with 60 MeV proton beam (dashed lines) and for 10 mm beam spot with 430 MeV/u carbon beam (solid lines)

gantry branch. The total number of vacuum sectors is 10. Each sector should be equipped with at least one turbomolecular pump and a vacuum gauge. The roughing pumps can be installed in a mobile station and used when pumping sector by sector. The choice of single type turbomolecular pump used across the facility is advised by CNAO [26]. They are easier to maintain and replace than ionic pumps.

Additional considerations for the vacuum system are as follows:

- The connection of the gantry should preferably be done using a windowless rotating interface to minimize beam particle scattering on the windows and on the air; the sector valve should be located upstream of this interface;
- The vacuum chamber of internal dump bumpers and of the scanning magnets should be ceramic to prevent Eddy currents and minimize the reaction time of the beam to the change of the magnetic field.

7 Beam instrumentation

The beam-sensing instruments allow to measure beam properties. The main challenge of SEEIIST HEBT is the large dynamic range required from the instruments, because of the high intensity of the beam stored in the synchrotron and beam extraction methods which include regular slow extraction (sub-nA of beam current), ,,fast slow extraction" (for FLASH, μA beam current) and fast extraction. The following beam measurement techniques should be envisaged:

- Beam current of the fast-slow and fast extracted beam can be measured using standard beam current transformers, and one such device should be installed in the common part

of HEBT. For regular slowly extracted beams the current measurement usually relays on the ionisation chambers of the beam delivery system. However other, noninvasive techniques, like reentrant cavity [27] or cryogenic current comparator, could be tested;

- Beam size, and hence beam optics, should be measured using scintillating screens, read by cameras with lenses equipped with remotely controlled aperture to maximize the dynamic range of the system. Such detectors will cover all beam intensities (maybe except of very low ones) and extraction modes. About 20 of these movable screens are needed to cover HEBT. This measure is destructive and it also provides information about beam position. A non-destructive information about beam size and position can be provided by a Ionization Profile Monitor installed in the common part of the HEBT. Additional information about beam position and size are provided by Multi-Wire Proportional Chambers installed in the nozzles of Therapeutic Rooms. They are crucial for very low intensities;

- Beam position monitors BPMs could be foreseen for fast-slow and fast extracted beams;

- Spill structure information is provided by gaseous nozzle detectors, but for slow extraction optimization studies additional, a much faster detector could be installed in the beam dump based on radiation hard sCVD diamond technology;

- Beam losses should be measured in critical locations, such as the extraction region, the beam chopper, and the beam dump, to provide additional information on the presence of the beam and quality of the extraction process.

8 Overall layout

The layout of the facility is shown in Figure 19 and it details the first concept presented in Figure 6. Without the vertical beam line (TR1V) and gantry, it contains 48 quadrupole magnets, 5 switching dipoles, and 6 fixed dipoles, and 3 or 4 pairs of scanning magnets (depending on the needs of experiments).

In addition, the HEBT also contains steering magnets. Vertical steering along the main line of HEBT is very important; the horizontal steering can be done, in many cases, using correction coils in the main dipoles. In total, around 5-8 horizontal and 11-16 vertical steerers will be needed.

The total length of the vacuum chambers in HEBT is about 200 meters.

9 Conclusions

A concept and a preliminary design of the SEEIIST High Energy Beam Transfer Lines foresees a large space in between the branching of the beam lines to particular treatment rooms or experimental ports. This space may be used for medical diagnostic equipment, but could be reduced by about 30% if further analysis finds that this space is too large. However, keeping this space large will future proof it, by not only allowing the installation of various additional medical equipment in the treatment rooms, but also the possible installation

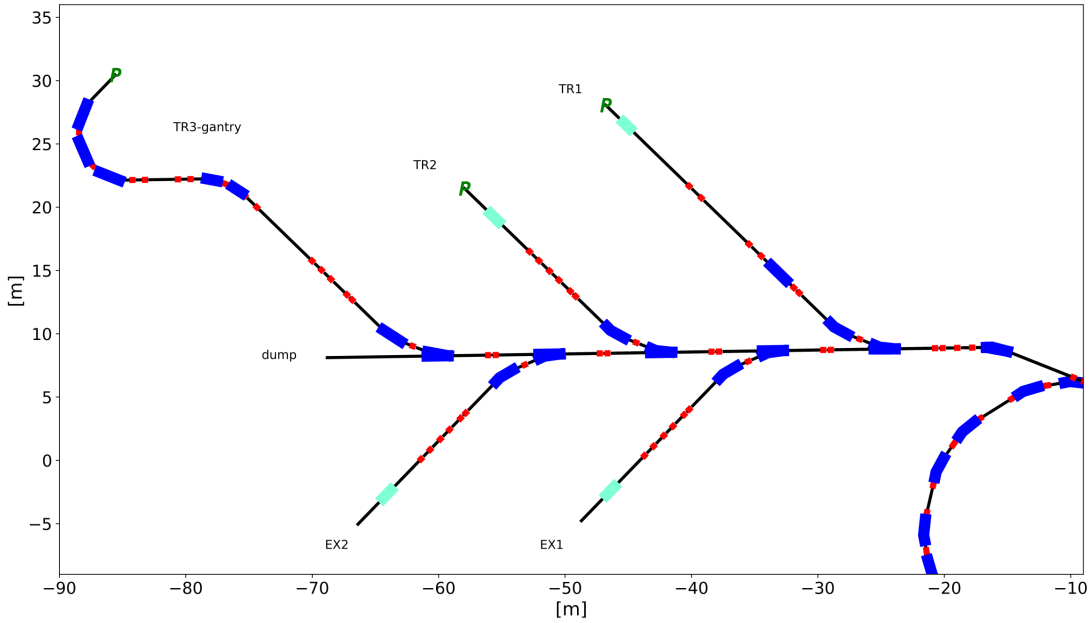

Figure 19: The layout of the facility HEBT lines. The light blue boxes are sets of scanning magnets.

of a second gantry in TR1 or TR2. The beam lines towards EX1 and EX2 experimental areas could be further subdivided to have additional experimental ports. The layout could be extended with additional beamlines. This design is versatile and adaptable to future experimental and treatment requirements.

The other key concepts behind the SEEIIST HEBT proposal are as follows:

- Separation of the experimental area from the treatment area;
- Dispersion suppressor section, which is almost indispensable when the beam is bent to both sides (i.e. experiments and treatment);
- Short bending section with a single central quadrupole in double-bend achromat configuration;
- Relying on the focusing sections to prepare the beam for treatments and for experiments.

In view of new, fast hadron therapy modalities like FLASH therapy, proposals have been made to speed up the beam abort times. These proposals include the double-chicane beam chopper or a beam chopper that makes use of the narrowness of the ,,bar of charge". Both of them should improve beam abort times down to 100 μs, what maybe critical for FLASH applications.

The design proposed here has been prepared without detailed knowledge of the boundary conditions which are not established yet. These conditions can significantly affect the final design, namely:

- The footprint and geometry of the available site;
- The available budget;
- The final lattice of the synchrotron;
- The list of experimental requirements.

Therefore, it is expected that numerous changes will be done to this design in the future. In authors' opinion the most important for the future study are the following aspects:

- Longer HEBT dipoles with a lower field but increased energy efficiency;
- Further optimization of Twiss β functions to minimize beam losses;
- Conversion of the beam dump into an experimental area;
- Further development of ultra-fast chopper based on a double-chicane or RF cavity;
- Convertion of the 90° beam line into 45° one.

In addition, the development of FLASH-compatible beam extraction mechanism is crucial and properties of produced beams may affect the aperture requirements of the HEBT.

10 Acknowledgements

Author would like to thank Elena Benedetto, Maurizio Vretenar, Marco Pullia, Christopher Kurfuerst, Ulrich Dorda and Phil Bryant for very useful discussions and remarks. Rebecca Taylor provided a MADX sequence of the PIMMS synchrotron extraction. Finally, several ideas arose from the discussion with students from South-East Europe: Milos Manojlovic and Mirsad Tunja, during their internships at CERN financed by Eddy Offermann and by IAEA. This work was supported by the European Union grant number 101008548 (HITRIplus) in the framework of the Horizon 2020 research and innovation program.

References

[1] P. J. Bryant, "Resonant extraction," *CERN Yellow Rep. School Proc.*, vol. 5, p. 315. 30 p, 2018.

[2] U. Weinrich, E. Sust, and R. Fuchs, "Assembly of the carbon beam gantry at the Heidelberg Ion Therapy (HIT) accelerator," in *Proc. of EPAC08, Genoa, Italy*, 2008.

[3] M. Benedikt, J. Gutleber, M. Palm, W. Pirkl, U. Dorda, and A. Fabich, "Overview of the MedAustron design and technology choices," Jun 2010. CERN-ATS-2010-116.

[4] L. Badano, M. Benedikt, P. J. Bryant, M. Crescenti, P. Holy, A. T. Maier, M. Pullia, S. Rossi, and P. Knaus, *Proton-Ion Medical Machine Study (PIMMS), part 1*. Mar 1999. https://cds.cern.ch/record/385378.

[5] E. Bressi, "Operation and Patient Treatments at CNAO Facility," *Conf. Proc. C*, vol. 1205201, pp. 3180–3184, 2012.

[6] T. Ohno, T. Kanai, S. Yamada, K. Yusa, M. Tashiro, H. Shimada, K. Torikai, Y. Yoshida, Y. Kitada, H. Katoh, T. Ishii, and T. Nakano, "Carbon ion radiotherapy at the Gunma University Heavy Ion Medical Center: New facility setup," *Cancers*, vol. 3, pp. 4046–4060, 2011.

[7] E. Takeshita, T. Furukawa, Y. Hara, Y. Kusano, S. Minohara, K. Mizushima, K. Noda, N. S. Saotome, Y. Saraya, R. Tansho, and S. Yamada, "Commissioning of Heavy-Ion Treatment Facility i-Rock in Kanagawa," in *Proc. of Heavy Ion Accelerator Technology Conference (HIAT2015), Yokohama, Japan, 7-11 September 2015*, pp. 130–133.

[8] "Osaka heavy ion therapy center." https://www.osaka-himak.or.jp. Accessed: 2022-01-30.

[9] U. Scheeler *et al.*, "Recommissioning of the Marburg Ion-beam Therapy Centre (MIT) Accelerator Facility," in *Proc. of International Particle Accelerator Conference (IPAC'16), Busan, Korea, May 8-13, 2016*.

[10] E. Benedetto, U. Amaldi, V. Bencini, M. Dosanjh, Y. Foka, D. Kaprinis, M. R. Khalvati, A. Lombardi, M. Sapinski, M. Vretenar, and X. Zhang, "Comparison of Accelerator Designs for an Ion Therapy and Research Facility," Dec 2020. CERN-ACC-NOTE-2020-0068 ; NIMMS-Note-001.

[11] "MADX - Methodical Accelerator Design." https://mad.web.cern.ch.

[12] P. J. Bryant, L. Badano, M. Benedikt, M. Crescenti, P. Holy, A. T. Maier, M. Pullia, S. Reimoser, S. Rossi, G. Borri, P. Knaus, F. Gramatica, M. Pavlovic, and L. Weisser, "Proton-Ion Medical Machine Study (PIMMS), 2," tech. rep., Aug 2000. CERN-PS-2000-007-DR.

[13] C. Kurfuerst. personal communication.

[14] H. Eickhoff, "HICAT-the Heavy Ion Cancer Therapy accelerator facility for the clinic in Heidelberg - Technical description," tech. rep., Dec 2000.

[15] M. Sapinski *et al.*, "Upgrade of GSI HADES Beamline in Preparation for High Intensity Runs," 5 2017. in Proc. of IPAC'17,Copenhagen, Denmark, paper TUPVA060.

[16] T. Haberer. private communication.

[17] L. Badano, M. Benedikt, P. Bryant, M. Crescenti, P. Holy, P. Knaus, A. Maier, M. Pullia, and S. Rossi, "Synchrotrons for hadron therapy: Part I," *Nuclear Instruments and Methods in Physics Research Section A: Accelerators, Spectrometers, Detectors and Associated Equipment*, vol. 430, no. 2, pp. 512–522, 1999.

[18] M. Sapinski, O. Geithner, C. Heßler, S. Reimann, P. Schütt, M. Vossberg, and B. Walasek-Höhne, "Measurements of the GSI transfer beam lines ion optics," in Proc. of IPAC'19, MOPGW024.

[19] J. Borburgh, B. Balhan, M. J. Barnes, T. Fowler, F. Hinterschuster, M. Hourican, T. Kramer, M. Palm, A. Prost, L. Sermeus, and T. Stadlbauer, "Design and Development of Kickers and Septa for MedAustron," in Proc. of IPAC'10, Kyoto, Japan, pp.THPEB032.

[20] M. G. Atanasov, "Design Optimization of the Fast Switched Chopper Dipole Magnet for the MedAustron Project," Sep 2014. PhD thesis presented on Oct 2, 2014.

[21] T. Stadlbauer, M. Barnes, M. Beerwald, U. Dirksen, R. Filippini, X. German, T. Kramer, F. Osmić, and P. Urschütz, "The Beam Chopper Power Converter for MedAustron: Safety by Design and Development," in Proc. of IPAC'15, Richmond, VA, USA, 3 - 8 May 2015, paper WEPMA002.

[22] U. Amaldi, E. Benedetto, S. Damjanovic, M. Dosanjh, M. Durante, P. Georgieva, T. Haberer, M. Plesko, M. Ristova, S. Rossi, N. Sammut, M. Sapinski, H. Schopper, H. Specht, R. Voss, M. Vretenar, and H. Wenninger, "South East European International Institute for Sustainable Technologies (SEEIIST)," tech. rep., 2020. Front. Phys., 29 January 2021.

[23] S. Jolly, H. Owen, M. Schippers, and C. Welsch, "Technical challenges for flash proton therapy," *Physica Medica*, vol. 78, pp. 71–82, 2020.

[24] U. Amaldi, N. Alharbi, E. Benedetto, P. Riboni, M. Vaziri, D. Aguglia, V. Ferrentino, G. Le Godec, M. Karppinen, D. Perini, E. Ravaioli, and D. Tommasini, "SIGRUM - A Superconducting Ion Gantry with Riboni's Unconventional Mechanics," Jun 2021. https://cds.cern.ch/record/2766876.

[25] S. Ghithan, G. Roy, and S. Schuh, "Design study of beam transport lines for BioLEIR facility at CERN," *Journal of Instrumentation*, vol. 12, pp. P09019–P09019, sep 2017.

[26] G. Venchi. personal communication.

[27] S. Srinivasan, P. Duperrex, and J. Schippers, "Reentrant Cavity Resonator as a Beam Current Monitor (BCM) for a Medical Cyclotron Facility," 2021. in Proc. of IBIC2020, WEPP05.